clock regulation of multiple outputs throughout development in *Arabidopsis thaliana*. *Development* **125,** 485–494 (1998).
16. Millar, A. J., Carré, I. A., Strayer, C. A., Chua, N.-H. & Kay, S. A. Circadian clock mutants in *Arabidopsis* identified by luciferase imaging. *Science* **267,** 1161–1163 (1995).
17. Alabadi, D. *et al.* Reciprocal regulation between *TOC1* and *LHY/CCA1* within the *Arabidopsis* circadian clock. *Science* **293,** 880–883 (2001).
18. Guo, H. W., Yang, W. Y., Mockler, T. C. & Lin, C. T. Regulation of flowering time by *Arabidopsis* photoreceptors. *Science* **279,** 1360–1363 (1998).
19. Johnson, E., Bradley, M., Harberd, N. P. & Whitelam, G. C. Photoresponses of light-grown *phyA* mutants of *Arabidopsis*. Phytochrome A is required for the perception of daylength extensions. *Plant Physiol.* **105,** 141–149 (1994).
20. Corbesier, L., Gadisseur, I., Silvestre, G., Jacqmard, A. & Bernier, G. Design in *Arabidopsis* of a synchronous system of floral induction by one long day. *Plant J.* **9,** 947–952 (1996).
21. Bünning, E. Die endogene Tagesrhthmik als Grundlage der photoperiodischen Reaktion. *Ber. Dtsch Bot. Ges.* **54,** 590–607 (1936).
22. Pittendrigh, C. S. & Minis, D. H. The entrainment of circadian oscillations by light and their role as photoperiodic clocks. *Am. Nat.* **98,** 261–294 (1964).
23. Pittendrigh, C. S. Circadian rhythms and the circadian organization of living systems. *Cold Spring Harbor Symp. Quant. Biol.* **25,** 159–184 (1960).
24. Yanovsky, M. J. & Kay, S. A. Signaling networks in the plant circadian system. *Curr. Opin. Plant Biol.* **4,** 429–435 (2001).
25. Blazquez, M. A. & Weigel, D. Independent regulation of flowering by phytochrome B and gibberellins in *Arabidopsis*. *Plant Physiol.* **120,** 1025–1032 (1999).

Supplementary Information accompanies the paper on *Nature*'s website (http://www.nature.com/nature).

Acknowledgements

We thank J. J. Casal, S. Harmer, P. Mas and F. Harmon for critical reading of the manuscript. This work was supported by an NIH grant to S.A.K. The work of M.J.Y. was initially supported by Conicet, Antorchas and the University of Buenos Aires and, more recently, by the Pew Foundation.

Competing interests statement

The authors declare that they have no competing financial interests.

Correspondence and requests for materials should be addressed to S.A.K. (e-mail: stevek@scripps.edu).

A regulatory cytoplasmic poly(A) polymerase in *Caenorhabditis elegans*

Liaoteng Wang*, Christian R. Eckmann†, Lisa C. Kadyk†‡, Marvin Wickens* & Judith Kimble*†

* *Department of Biochemistry, University of Wisconsin-Madison, Madison, Wisconsin 53706, USA*
† *Howard Hughes Medical Institute, 433 Babcock Drive, University of Wisconsin-Madison, Madison, Wisconsin 53706, USA*

Messenger RNA regulation is a critical mode of controlling gene expression. Regulation of mRNA stability and translation is linked to controls of poly(A) tail length[1,2]. Poly(A) lengthening can stabilize and translationally activate mRNAs, whereas poly(A) removal can trigger degradation and translational repression. Germline granules (for example, polar granules in flies, P granules in worms) are ribonucleoprotein particles implicated in translational control[3]. Here we report that the *Caenorhabditis elegans* gene *gld-2*, a regulator of mitosis/meiosis decision and other germline events[4], encodes the catalytic moiety of a cytoplasmic poly(A) polymerase (PAP) that is associated with P granules in early embryos. Importantly, the GLD-2 protein sequence has diverged substantially from that of conventional eukaryotic PAPs, and lacks a recognizable RRM (RNA recognition motif)-like domain. GLD-2 has little PAP activity on its own, but is stimulated *in vitro* by GLD-3. GLD-3 is also a developmental regulator, and belongs to the Bicaudal-C family of RNA binding proteins[5]. We suggest that GLD-2 is the prototype for a class of regulatory cytoplasmic PAPs that are recruited to specific mRNAs by a binding partner, thereby targeting those mRNAs for polyadenylation and increased expression.

We cloned the *gld-2* gene and analysed its transcripts (Fig. 1). The *gld-2* genomic region was identified by mutant rescue and RNA-aided interference (RNAi; see Methods) as well as elucidation of the molecular lesions in two *gld-2* mutants (see below). The *gld-2* gene encodes multiple mRNAs (Fig. 1a, b). A 5′ probe detected a 4.7-kilobase (kb) band in wild-type poly(A)$^+$ RNAs, but not in RNA from germline-less mutants (Fig. 1b, left). Therefore, this 4.7-kb mRNA appears to be germline-specific. Middle and 3′ probes detected two somatic *gld-2* RNAs, of 4.6 and 4.0 kb (Fig. 1b, middle and right). These smaller *gld-2* mRNAs harbour distinct 5′ terminal exons spliced to common exons (Fig. 1a). Two *gld-2* mutations identified genetically[4] carried lesions in common exons: a predicted null mutant, *gld-2(q497)*, is a premature nonsense codon, and *gld-2(h292)* is a missense mutation (E875K) (Fig. 1a).

Because of our interest in *gld-2* germline functions, we focused on its 4.7-kb mRNA. Northern analysis (Fig. 1b, left) showed that this mRNA was abundant in embryos, fourth larval stages (L4s) and adults (Fig. 1c); *in situ* hybridization showed that it was abundant in the meiotic pachytene region and in oogenesis (Fig. 1d, e), but decreased during spermatogenesis (Fig. 1e). We did not detect the mRNA in putative null mutant *gld-2(q497)* (Fig. 1f), or with a sense-strand probe (anti-5′) (Fig. 1g). Therefore, *gld-2* is expressed

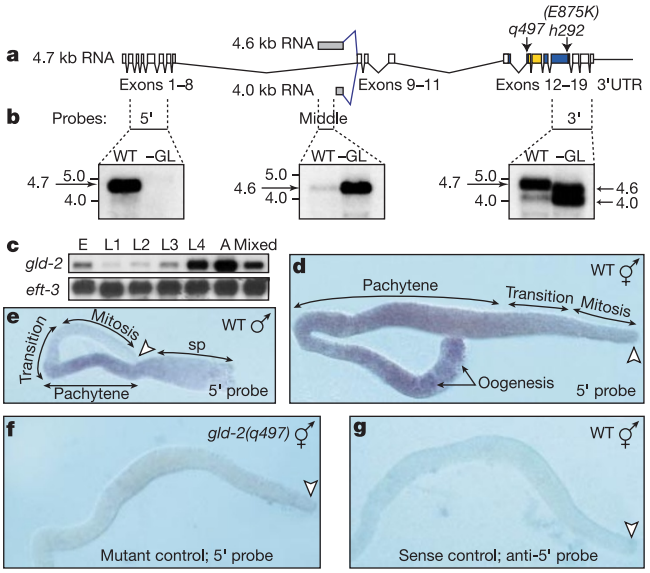

Figure 1 The *gld-2* gene and its transcripts. **a**, *gld-2* exon/intron structure. Exons, open boxes; introns, thin lines. Colour coding as in Fig. 2b. **b**, Top, probes (see Methods). Bottom, northern blots of poly(A)$^+$ RNAs from mixed stage wild-type (WT) animals or from *glp-1* mutant adults with no germ line (−GL). Size markers in kb. Arrows, *gld-2* transcripts. Sizes of *gld-2* transcripts on northern blots (4.7 kb, 4.6 kb and 4.0 kb) correspond to sizes predicted by cDNA analyses (4,533 nt, 4,273 nt and 3,691 nt, excluding the poly(A) tail). **c**, Developmental expression of *gld-2* mRNA. Northern blot of poly(A)$^+$ RNAs from staged animals. E, embryo; L1–L4, first–fourth larval stage; A, adult; mixed, mixed stages. Above, 5′ probe, Fig. 1b; below, loading control. **d**–**g**, *In situ* hybridization of dissected germ lines. **d**–**f**, 5′ probe, Fig. 1b; open arrowhead, distal end of germ line. **d**, Germ line of wild-type hermaphrodite adult. **e**, Germ line of wild-type male adult; sp, spermatogenesis; WT, wild type; **f**, germ line of *gld-2(q497)* homozygous mutant adult; **g**, germ line of wild-type hermaphrodite adult, probed with sense strand of cDNA fragment covering exons 2–8 (5′ probe, 1b).

‡ Present address: Exelixis, Inc., 170 Harbor Way, PO Box 511, So. San Francisco, California 94083-0511, USA.

in the germ line and is developmentally regulated.

Database searches revealed that GLD-2 protein belongs to the DNA polymerase β-like superfamily of nucleotidyltransferases (NT) (Fig. 2a; refs 6, 7). Specifically, GLD-2 is a group 2 NT member, including DNA polymerase σ of *Saccharomyces cerevisiae* (also known as pol κ and Trf4p) and eukaryotic PAPs (Fig. 2a). GLD-2 architecture and sequence is divergent from that of canonical PAPs (Fig. 2b, d), but similar to a different cluster of NT family members (Fig. 2e). GLD-2 contains three critical carboxylate side chains essential for catalytic activity (Fig. 2c, red) present in all DNA polymerase β superfamily members; furthermore, GLD-2 possesses putative ATP-interacting residues (Fig. 2c, green; Fig. 2d, green). Classical PAPs have a catalytic region (Fig. 2c, gold), a 'central' domain (Fig. 2c, blue), and an RRM-like region (Fig. 2c, violet)[8,9]. By sequence comparison, GLD-2 harbours catalytic and central domains (Fig. 2b, d, colour-coded overlines), but is highly diverged from classical eukaryotic PAPs, including *C. elegans* PAP-1 (C. Luitjens and M.W., unpublished results) (Fig. 2d). Classical PAPs show extensive amino-acid conservation among themselves, but limited conservation with GLD-2 (Fig. 2d, black and grey boxes). Outside its catalytic and central domains, GLD-2 shares little similarity to canonical PAPs; in particular, GLD-2 has no apparent RRM-like region (Fig. 2b), which is thought to be critical for PAP RNA binding[8,9]. Therefore, GLD-2 shares some key features with classical PAPs, but is divergent in motif architecture and amino acid sequence.

To examine GLD-2 protein, we generated polyclonal antibodies to the amino-terminal region (Fig. 2b) and detected a prominent protein of relative molecular mass 125,000 (M_r 125K) on western blots (Fig. 3a, lanes 1, 4, 5). This protein, which corresponds in size to the predicted product of the germline *gld-2* mRNA, was detected in *gld-2(h292)* homozygotes and *gld-2(q497)/+* heterozygotes (Fig. 3a, lanes 6, 7), but not in *gld-2(q497)* homozygotes (Fig. 3a, lane 8). Pre-immune serum did not recognize this band, but detected others that served as a loading control (not shown). We conclude that the α-GLD-2 antibody recognizes GLD-2, that the *gld-2(h292)* mutant produces a nearly wild-type level of protein and that *gld-2(q497)* is a strong loss-of-function or null allele.

By immunocytochemistry, GLD-2 was found to be predominantly cytoplasmic in both germ line (Fig. 3b) and early embryo (Fig. 3c). Within the germ line, GLD-2 was detectable in the mitotic region and became abundant during pachytene and oogenesis (Fig. 3b). GLD-2 decreased during spermatogenesis in both sexes, and was undetectable in mature sperm (not shown). In early embryos, GLD-2 was diffuse in the cytoplasm of early P0 embryos, co-localized with P granules in late P0 embryos and remained associated with P granules in germline blastomeres (Fig. 3c, not shown). P granules are essential for germline development[3,10]. In ~100-cell embryos, GLD-2 was undetectable.

Given its presence in oocytes and early embryos, we tested whether GLD-2 was required for embryogenesis. To deplete both maternal and zygotic *gld-2* mRNAs, wild-type adult hermaphrodites were treated with double-stranded RNA corresponding to either the *gld-2* germline-specific region (exons 2–8) or its common region (exons 16–18) to produce *gld-2(RNAi)* embryos (see Methods). In both cases, most *gld-2(RNAi)* embryos failed to hatch (99%, $n > 500$ in 26–36 h period after treatment). To visualize chromosomes in *gld-2(RNAi)* embryos, we used a strain carrying a histone::GFP transgene (AZ212)[11]. Whereas mock-treated AZ212 embryos cleaved normally (Fig. 3d), *gld-2(RNAi)* AZ212 embryos did not cleave and possessed malformed nuclei in clusters (Fig. 3e). We conclude that *gld-2* activity is required for embryogenesis, and that GLD-2 protein co-localizes with P granules.

A specific interaction between GLD-2 and another germline regulator, GLD-3 (ref. 5), was discovered in yeast two-hybrid screens. Specifically, using GLD-2 as 'bait', 2,000,000 transformants

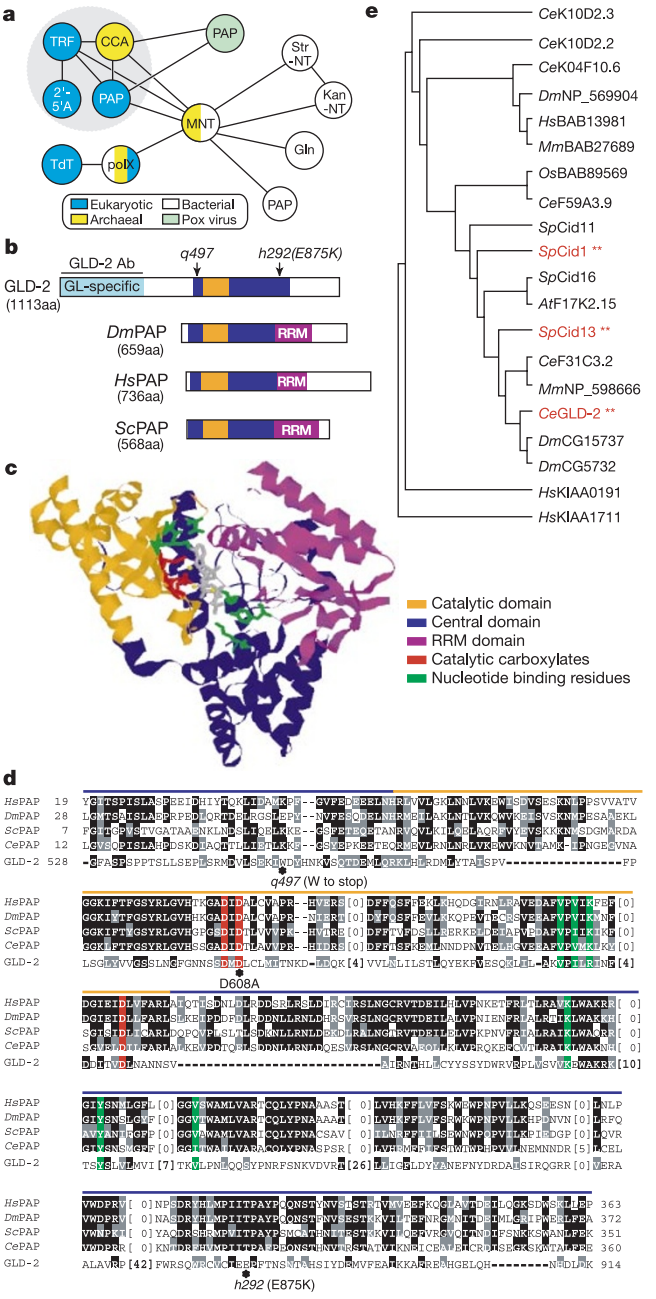

Figure 2 GLD-2 belongs to the polymerase β nucleotidyltransferase superfamily. **a**, The polymerase β superfamily (adapted from ref. 7). Small colour-coded circles, families; large grey circle, group 2 families. CCA, CCA-adding enzymes; 2′-5′ A, 2′-5′ oligoA synthetases; TRF, Trf4p-like proteins; other acryonyms as in ref. 7. **b**–**d**, Colour coding based on crystal structures of bovine and yeast PAPs[8,9]. Gold, catalytic domain; blue, central domain; violet, RRM domain. **b**, GLD-2 and PAP domains compared. *Drosophila* (*Dm*), human (*Hs*) and yeast (*Sc*). GLD-2 domains identified by Pfam search[27]. aa, amino acid **c**, Bovine PAP 3D structure, with key residues shown in stick form (adapted from ref. 8). Created by Rasmol based on PDB file 1F5A (for bovine PAP). **d**, Amino-acid sequence alignment of GLD-2 and PAP core regions based on clustalW output[28] and polymerase β superfamily analyses[29]. Mutants designated below. Red, catalytic residues; green, required for ATP binding. **e**, Unrooted tree of GLD-2 and its homologues, created with PHYLIP programs[30], based on ClustalW alignment using parsimony. Species are: *Ce*, *C. elegans*; *Dm*, *Drosophila*; *Hs*, human; *Mm*, mouse; *Os*, rice; *Sp*, *S. pombe*; *At*, *Arabidopsis*. Only homologues with *E*-values less than 1×10^{-10} in the first PSI blast were used; tree was built using the catalytic and central domain sequences as in **d** (GLD-2 amino acids 528–914 and corresponding sequences of its homologues). Cid1 and GLD-2 (shown red) both function in cell cycle control; Cid13 (shown red) is involved in the replication stress response[22]; functions of others are unknown.

were screened and 30 *gld-3* cDNAs (T07F8.3) found; using GLD-3 as bait, 1,500,000 transformants were screened and 94 *gld-2* cDNAs recovered. To identify the region of GLD-2 critical for GLD-3 binding, GLD-2 variants were assayed for GLD-3 interaction. A GLD-2 fragment comprising both catalytic and central domains was essential (amino acids 544–924) (Fig. 4a). A GLD-2-E875K mutant, designed after *gld-2(h292)*[4], interacted poorly with GLD-3 (Fig. 4a, E875K and Δ7). Indeed, β-galactosidase activity was reduced 7- to 16-fold by GLD-2(h292)-E875K (Fig. 4a, compare for example Δ2 to Δ7), but GLD-2 levels were equivalent (Fig. 4b). Importantly, GLD-2-E875K was present at normal levels in *C. elegans* (Fig. 3a, lane 6), even though it disrupts *gld-2* function. We conclude that GLD-2 binds specifically to GLD-3, and that GLD-2-E875K is defective in GLD-3 binding. Therefore, the GLD-2/GLD-3 interaction appears to be important for development.

Given its sequence similarity to nucleotidyltransferases and its cytoplasmic location, we considered that GLD-2 might be a cytoplasmic PAP, even though its architecture and sequence diverged substantially from classical PAPs. To test this idea, we initially assayed incorporation of radiolabelled ATP into an RNA substrate. Specifically, GLD-2 was translated *in vitro*, either on its own or together with GLD-3. The *in vitro* translation mixture was incubated with ^{32}P-ATP and an unlabelled poly(A) substrate, and incorporation of label into acid-insoluble material was measured (see Methods). GLD-2 on its own had low activity, whereas GLD-3 had none; however, GLD-2 and GLD-3 together gave a robust response (Fig. 4c). We also measured incorporation in three control reactions (no protein and two GLD-2 mutants together with GLD-3). GLD-2-D608A was designed to abolish the catalytic site (Fig. 2c) and GLD-2-E875K was used to disrupt GLD-3 binding (Fig. 4a). The control reactions yielded no measurable ^{32}P-ATP incorporation (Fig. 4c). From these experiments, we argue that GLD-2 is in fact a nucleotidyltransferase and that both its predicted active site and GLD-3 binding region are essential for enzymatic activity.

We next analysed the products of the GLD-2/GLD-3 nucleotidyltransferase activity by electrophoresis and autoradiography (Fig. 4d). To this end, reactions were done as described above, except that $C_{35}A_{10}$ (see Methods) was used as substrate. Two exposures of the same autoradiogram are shown (Fig. 4d). As a marker, $C_{35}A_{10}$ was 3′ end-labelled with cordycepin triphosphate ([α-^{32}P] 3′ dATP) ($C_{35}A_{10}$*dA; Fig. 4d left, lane 1). GLD-2 by itself exhibited modest incorporation from ATP into bands that extended the substrate by only one or a few nucleotides (Fig. 4d left, lane 2). In contrast, GLD-2 plus GLD-3 stimulated incorporation, resulting in more product with a 'ladder' of poly(A) extending the substrate more than 30 adenosines (Fig. 4d, lane 4). The ladder mimics the activity of bovine nuclear PAP (bPAP), but is less efficient (Fig. 4d, compare lanes 4 and 7). This difference may reflect the fact that bovine PAP acts as a monomer, whereas GLD-2 PAP activity is dependent on the interaction of two dilute proteins. Furthermore, although abundant products had only two or three nucleotides added (asterisks in Fig. 4d, lane 4), more-minor products had as many as 70 additional nucleotides. We conclude that GLD-2/GLD-3 can catalyse the addition of a poly(A) tail to an RNA substrate.

Four controls support the conclusion that GLD-2 is a PAP. First, GLD-2 PAP activity was abolished by a site-directed mutation in the inferred active site (D608A) (Fig. 4d, lane 5). Importantly, GLD-2-D608A level is equivalent to that of wild-type GLD-2 in the same assay (Fig. 4d SDS–polyacrylamide gel electrophoresis, SDS–PAGE, compare lanes 4 and 5). Thus, the GLD-2 putative active site is required for AMP addition *in vitro*. Second, GLD-2 PAP activity was abolished by the E875K mutation (Fig. 4d, lane 6), which disrupts GLD-2/GLD-3 binding (Fig. 4a). The GLD-2-E875K level was equivalent to wild-type GLD-2 (Fig. 4d, compare lanes 4 and 6). Third, GLD-2-dependent incorporation is substrate dependent and requires ATP (not shown). Thus, replacement of ATP with GTP, CTP or UTP did not yield incorporation onto the substrate. Finally, products produced by GLD-2 plus GLD-3 were selectively retained on oligo(dT) cellulose, suggesting they were polyadenylated (not shown).

The GLD-2/GLD-3 enzyme represents a new type of poly(A) polymerase (Fig. 5). Canonical PAPs, which include nuclear and cytoplasmic enzymes, are all closely related[12–15]; they are monomeric and possess three key domains (Fig. 5, left)[8,9]. By contrast, GLD-2 appears to function as a heterodimer (Fig. 5, right). GLD-2 harbours the catalytic and central domains; GLD-3 has five consecutive K homology (KH)-related motifs[5] which may, at least in

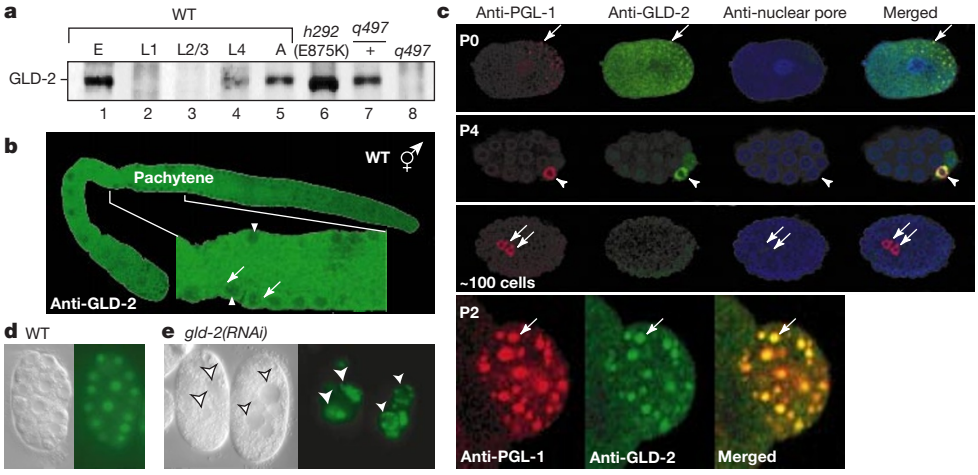

Figure 3 The GLD-2 protein. Polyclonal anti-GLD-2 antibodies were affinity purified. **a**, Western blot of proteins from wild-type embryos (E), larvae (L1–L4), and adults (A) (lanes 1–5), and adults of genotype *gld-2(h292)/gld-2(h292)* (lane 6), *gld-2(q497)/gld-2(+)* (lane 7), and *gld-2(q497)/gld-2(q497)* (lane 8). **b**, GLD-2 protein is in germline cytoplasm. Extruded WT adult hermaphrodite germ line; GLD-2 is abundant in pachytene region and oocytes. Magnified view shows lack of GLD-2 in nuclei (arrowheads) and presence of GLD-2 in granular form (arrows). A control *gld-2(q497)* extruded germ line showed no anti-GLD-2 staining (not shown). **c**, GLD-2 protein is associated with P granules in early embryos. Embryos stained with antibody to P granule marker, PGL-1[10], to GLD-2, and to nuclear pore antigen. Top, late P0 embryo, GLD-2 co-localizes with P granules; second panel down, 28-cell embryo, P4, white arrowhead; third panel, ~100-cell embryo, germline precursor cells, Z2 and Z3, arrows; bottom, magnified view of P2 blastomere to show PGL-1 and GLD-2 co-localization (arrows). **d**, **e**, Transgenic strain AZ212. Left, Nomarski image; right, nuclei visualized by histone::GFP maker. Both control and *gld-2(RNAi)* embryos are of approximately same age. **d**, Mock injected control. **e**, *gld-2(RNAi)*.

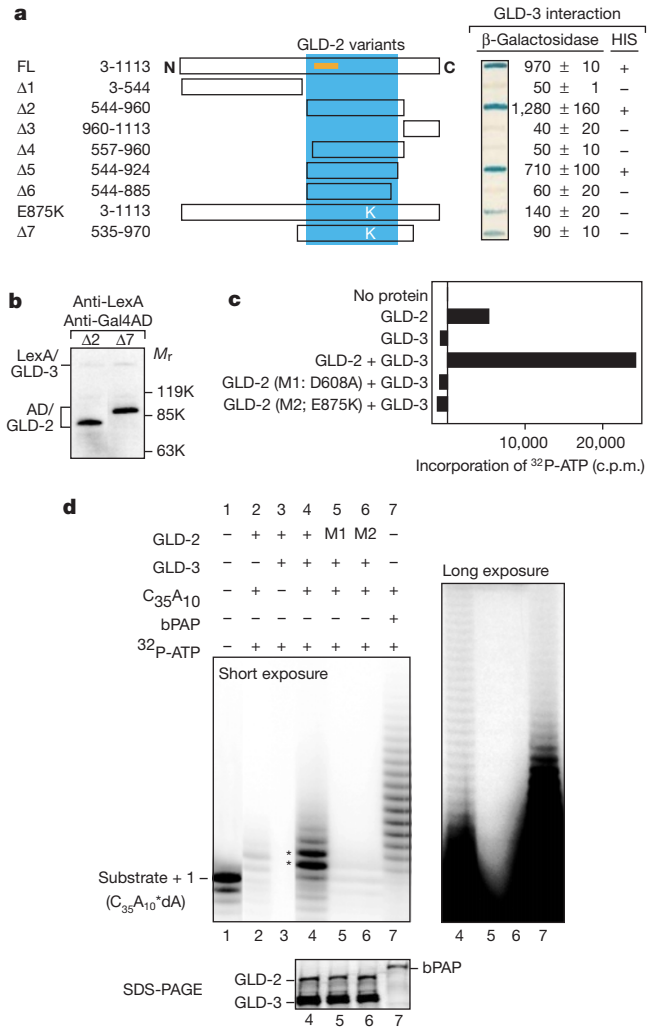

Figure 4 GLD-2/GLD-3 is a new type of poly(A) polymerase. **a**, Left, GLD-2 deletions used in yeast two-hybrid assays to map region of GLD-3 interaction. Right, results of both filter and liquid β-galactosidase assays as well as a growth assay (HIS). **b**, GLD-2 fragments were expressed at similar level. Western blot, Δ2 and Δ7 fragments as in **a**. **c**, Nucleotidyltransferase assay. Incorporation of ^{32}P-ATP was measured in reticulocyte lysates programmed with plasmids encoding GLD-2, GLD-3 or variants. Data reported as c.p.m., not molar quantities, because ATP concentration in lysate was not known. The lysate exhibits a background incorporation (10,000 c.p.m.) independent of GLD-encoding plasmids, which has been subtracted here. In the experiment shown, 1 mM $MnCl_2$ was added to the lysate; similar experiments with added $MgCl_2$ reduced incorporation four-fold. **d**, Poly(A) polymerase assay. Reaction products analysed on a 12% sequencing gel and visualized by autoradiography. Left, shorter exposure; right, longer exposure. Below, SDS–PAGE showing that proteins were expressed at similar levels. M1, D608A; M2, E875K; $C_{35}A_{10}$, substrate; bPAP, bovine poly(A) polymerase.

part, substitute for the RRM domain of classical PAPs. In the simplest view, GLD-2 and GLD-3 act together as a heterodimer to accomplish what classical PAPs do on their own. However, we suggest that GLD-2 is tailored for a more regulatory role than that typical of classical PAPs. For example, GLD-3 is likely to provide sequence specificity to the GLD-2 catalytic activity, and GLD-2 may interact with additional partners to expand its repertoire of regulation.

GLD-2 and GLD-3 are likely to function together during nematode development. First, GLD-2 and GLD-3 have similar, albeit not identical, functions in germline development and embryogenesis (refs 4, 5, and this work). Second, both are cytoplasmic and associated with P granules (ref. 5, this work), large complexes of

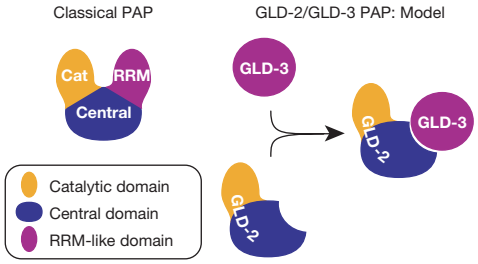

Figure 5 Model for architecture of GLD-2/GLD-3 rcPAP enzyme. Left, classical PAPs. Right, speculative architecture of GLD-2/GLD-3. Domains colour coded as in Fig. 2.

RNA and protein that are critical for germline development[3,10]. GLD-2 and GLD-3 may polyadenylate mRNAs associated with P granules (for example, *nos-2*; ref. 16) or may be stored there for segregation to germline blastomeres. GLD-2 may be targeted to specific mRNAs by GLD-3, which is a Bic-C family KH protein[5]. Other KH proteins (FMRP, NOVA, hnRNPK) bind RNAs through sequence-specific interactions[17–20]. GLD-2 may also be targeted to specific mRNAs indirectly via the interaction of GLD-3 with FBF[5]. FBF is a sequence-specific RNA-binding protein and member of the PUF family[21]. PUF proteins appear to repress mRNAs by promoting poly(A) removal[21]. GLD-3 antagonizes FBF[5], and works with GLD-2 to promote poly(A) addition (this work). Therefore, GLD-2/GLD-3 may switch FBF from a repressive to an activating mode.

Regulatory cytoplasmic PAPs of the GLD-2/GLD-3 class may be common. Within the large superfamily of DNA polymerase β-like nucleotidyltransferases, several are closely related to GLD-2 (Fig. 2e). To date, most have no assigned function, but *Schizosaccharomyces pombe* Cid13 and Cid1 appear to be rcPAPs[22,31]. The similarity between GLD-2 and Cid1 is particularly striking, as both are involved in cell cycle control. GLD-2 promotes entry into meiosis at the expense of mitosis[4], and Cid1 inhibits mitosis[23]. We suggest that GLD-2 and Cid1 may in fact be components of an ancient regulatory circuit controlling the cell cycle, and that other GLD-2 relatives may similarly be regulatory cytoplasmic PAPs. □

Methods

Molecular cloning of *gld-2*

Three-factor mapping places *gld-2* 0.05 map unit to the right of *bli-4*. Cosmids in this region were injected into strain JK1716 [*bli-4(e937) gld-2(q497)/dpy-5(e61) unc-13(e51)*] or strain JK1732 [*bli-4(e937) gld-2(h292)/dpy-5(e61) unc-13(e51)*]. Cosmid ZC308 gave ~4% germline rescue.

Transcript analyses

Northern blots were performed as described[24]. Templates for making RNA probes (*gld-2* 5′, middle, 3′; *eft-3*) were made by polymerase chain reactions (PCRs) from pJK830, pJK831, pJK832 and pBluescript-*eft-3* (gift from P. Anderson). To determine the *gld-2* 3′ end, semi-nested PCR was performed using λAE.1, a *C. elegans* mixed-stage oligo(dT) primed complementary DNA library (gift from A. Puoti). One PCR product was confirmed and sequenced. A stretch of 22 As was found at the end of the 3′ untranslated region (UTR). To determine the *gld-2* 5′ ends, reverse transcriptions (RT) were performed using SuperScript II Reverse Transcriptase (Gibco BRL) and poly(A)$^+$ RNA from either wild-type mixed-stage worms or *glp-1(q224)* mutants raised at 25 °C, which have no germ line. The resultant cDNAs were then used as templates for semi-nested PCR with SL1 (a trans-spliced leader in *C. elegans*) as the constant 5′ primer. All PCR products were cloned into pSTBlue-1 and sequenced. The 4.7-kb mRNA is SL1 trans-spliced, comprises 19 exons including an 86-nucleotide 5′ UTR and 1,105-nucleotide 3′ UTR.

Antibody production, western blot and immunocytochemistry

Polyclonal antibodies were generated from rabbits using a keyhole limpet haemocyanin (KLH)-conjugated peptide corresponding to GLD-2 amino acids 108–127 (Genemed Synthesis) or from rats using a GST–GLD-2 fusion protein carrying amino acids 13–330 of GLD-2. Rabbit anti-PGL-1 antibody was a gift from S. Strome. Monoclonal antibody 414, the anti-nuclear pore monoclonal, was purchased from BABCO. Western blots were performed using the GLD-2 peptide antibody as described[24]. Immunocytochemistry followed published procedures[25] using the GST–GLD-2 fusion-protein antibody, which was specific for GLD-2 as demonstrated on *gld-2(q497)* extruded germ lines and *gld-2(RNAi)* embryos.

RNAi

Double-stranded RNAs (dsRNAs) were made using *gld-2* cDNAs (pJK830, exons 2–8 or pJK831, exons 16–18) as templates. Young adults were either injected with 2 $\mu g\,\mu l^{-1}$ *gld-2* dsRNA or soaked in 10 μl of 2 $\mu g\,\mu l^{-1}$ *gld-2* dsRNA for 12 h at 20 °C or mock-treated by injection with M9 buffer. Embryos were collected at defined intervals after treatment and processed together.

Poly(A) polymerase assay

Proteins were *in vitro* translated using the TNT coupled transcription–translation system (Promega), and assayed using buffer conditions essentially as described[26]. For scintillation counting, poly(A) (Roche) was used as substrate. For gel assays, we used RNA oligo, $C_{35}A_{10}$ (Dharmacon), a 45-nucleotide and supplemental 1 mM $MgCl_2$. Products were analysed on 12% sequencing gels.

Received 8 May; accepted 16 July 2002; doi:10.1038/nature01039.

1. Richter, J. D. in *Translational Control of Gene Expression* (eds Sonenberg, N., Hershey, J. W. B. & Mathews, M. B.) 785–805 (Cold Spring Harbor Laboratory Press, Cold Spring Harbor, New York, 2000).
2. Wickens, M., Goodwin, E. B., Kimble, J., Strickland, S. & Hentze, M. W. in *Translational Control of Gene Expression* (eds Sonenberg, N., Hershey, J. W. B. & Mathews, M. B.) 295–370 (Cold Spring Harbor Laboratory Press, Cold Spring Harbor, New York, 2000).
3. Seydoux, G. & Strome, S. Launching the germline in *Caenorhabditis elegans*: regulation of gene expression in early germ cells. *Development* **126,** 3275–3283 (1999).
4. Kadyk, L. C. & Kimble, J. Genetic regulation of entry into meiosis in *Caenorhabditis elegans*. *Development* **125,** 1803–1813 (1998).
5. Eckmann, C., Kraemer, B., Wickens, M. & Kimble, J. GLD-3, a Bicaudal-C homolog that represses FBF to control germline sex determination in *C. elegans*. *Dev. Cell* (in the press).
6. Holm, L. & Sander, C. DNA polymerase β belongs to an ancient nucleotidyltransferase superfamily. *Trends Biochem. Sci.* **20,** 345–347 (1995).
7. Aravind, L. & Koonin, E. V. DNA polymerase β-like nucleotidyltransferase superfamily: identification of three new families, classification and evolutionary history. *Nucleic Acids Res.* **27,** 1609–1618 (1999).
8. Martin, G., Keller, W. & Doublie, W. Crystal structure of mammalian poly(A) polymerase in complex with an analog of ATP. *EMBO J.* **19,** 4193–4203 (2000).
9. Bard, J. *et al.* Structure of yeast poly(A) polymerase alone and in complex with 3′-dATP. *Science* **289,** 1346–1349 (2000).
10. Kawasaki, I. *et al.* PGL-1, a predicted RNA-binding component of germ granules, is essential for fertility in *C. elegans*. *Cell* **94,** 635–645 (1998).
11. Praitis, V., Casey, E., Collar, D. & Austin, J. Creation of low-copy integrated transgenic lines in *Caenorhabditis elegans*. *Genetics* **157,** 1217–1226 (2001).
12. Colgan, D. F. & Manley, J. L. Mechanism and regulation of mRNA polyadenylation. *Genes Dev.* **11,** 2755–2766 (1997).
13. Kashiwabara, S.-i. *et al.* Identification of a novel isoform of poly(A) polymerase, TPAP, specifically present in the cytoplasm of spermatogenic cells. *Dev. Biol.* **228,** 106–115 (2000).
14. Kyriakopoulou, C. B., Nordvarg, H. & Virtanen, A. A novel nuclear human poly(A) polymerase (PAP), PAPγ. *J. Biol. Chem.* **276,** 33504–33511 (2001).
15. Topalian, S. L. *et al.* Identification and functional characterization of neo-poly(A) polymerase, an RNA processing enzyme overexpressed in human tumors. *Mol. Cell. Biol.* **21,** 5614–5623 (2001).
16. Subramaniam, K. & Seydoux, G. *nos-1* and *nos-2*, two genes related to *Drosophila nanos*, regulate primordial germ cell development and survival in *Caenorhabditis elegans*. *Development* **126,** 4861–4871 (1999).
17. Jensen, K. B., Musunuru, K., Lewis, H. A., Burley, S. K. & Darnell, R. B. The tetranucleotide UCAY directs the specific recognition of RNA by the Nova K-homology 3 domain. *Proc. Natl Acad. Sci. USA* **97,** 5740–5745 (2000).
18. Brown, V. *et al.* Microarray identification of FMRP-associated brain mRNAs and altered mRNA translational profiles in fragile X syndrome. *Cell* **107,** 477–487 (2001).
19. Darnell, J. C. *et al.* Fragile X mental retardation protein targets G quartet mRNAs important for neuronal function. *Cell* **107,** 489–499 (2001).
20. Ostareck, D. H. *et al.* mRNA silencing in erythroid differentiation: hnRNP K and hnRNP E1 regulate 15-lipoxygenase translation from the 3′ end. *Cell* **89,** 597–606 (1997).
21. Wickens, M., Bernstein, D. S., Kimble, J. & Parker, R. A PUF family portrait: 3′UTR regulation as a way of life. *Trends Genet.* **18,** 150–157 (2002).
22. Saitoh, S. *et al.* Cid13 is a cytoplasmic poly(A) polymerase that regulates ribonucleotide reductase mRNA. *Cell* **109,** 563–573 (2002).
23. Wang, S. W., Toda, T., MacCallum, R., Harris, A. L. & Norbury, C. Cid1, a fission yeast protein required for S-M checkpoint control when DNA polymerase delta or epsilon is inactivated. *Mol. Cell. Biol.* **20,** 3234–3244 (2000).
24. Sambrook, J., Fritsch, E. F. & Maniatis, T. (ed.) *Molecular Cloning: A Laboratory Manual* (Cold Spring Harbor Laboratory Press, New York, 1989).
25. Crittenden, S. L. & Kimble, J. in *Cell: A Laboratory Manual* (eds Spector, D., Goldman, R. & Leinwand, L.) 108.1–108.9 (Cold Spring Harbor Laboratory Press, Cold Spring Harbor, New York, 1998).
26. Lingner, J., Radtke, I., Wahle, E. & Keller, W. Purification and characterization of poly(A) polymerase from *Saccharomyces cervisiae*. *J. Biol. Chem.* **266,** 8741–8746 (1991).
27. Bateman, A. *et al.* The Pfam protein families database. *Nucleic Acids Res.* **30,** 276–280 (2002).
28. Thompson, J. D., Higgins, D. G. & Gibson, T. J. CLUSTAL W: improving the sensitivity of progressive multiple sequence alignment through sequence weighting, positions-specific gap penalties and weight matrix choice. *Nucleic Acids Res.* **22,** 4673–4680 (1994).
29. Gough, J., Karplus, K., Hughey, R. & Chothia, C. Assignment of homology to genome sequences using a library of hidden Markov models that represent all proteins of known structure. *J. Mol. Biol.* **313,** 903–919 (2001).
30. Felsenstein, J. *PHYLIP (Phylogeny Inference Package) Version 3.5c* (Department of Genetics, Univ. Washington, Seattle, 1993).
31. Read, R. L., Martinho, R. G., Wang, S.-W., Carr, A. M. & Norbury, C. J. Cytoplasmic poly(A) polymerases mediate cellular responses to S phase arrest. *Proc. Natl Acad. Sci. USA* (in the press).

Acknowledgements

We thank R. Read and C. Norbury for sharing unpublished observations, and S. Crittenden for comments on the manuscript. C.E. was supported by the Human Frontier Science Program, L.K. was supported by the American Cancer Society, J.K. is an investigator with the Howard Hughes Medical Institute, and M.W. is supported by the National Institutes of Health.

Competing interests statement

The authors declare that they have no competing financial interests.

Correspondence and requests for materials should be addressed to J.K. (e-mail: jekimble@facstaff.wisc.edu). The GenBank accession number of the GLD-2 cDNA sequence is AY125085.

Forkhead transcription factor FOXO3a protects quiescent cells from oxidative stress

Geert J. P. L. Kops*†, Tobias B. Dansen‡, Paulien E. Polderman*, Ingrid Saarloos*, Karel W. A. Wirtz‡, Paul J. Coffer§, Ting-T. Huang‖, Johannes L. Bos*, René H. Medema¶# & Boudewijn M. T. Burgering*#

** Department of Physiological Chemistry, University Medical Center Utrecht and Center for Biomedical Genetics, 3584 CG Utrecht, The Netherlands*
‡ Department of Biochemistry of Lipids, Institute of Biomembranes, Utrecht University, 3584 CH Utrecht, The Netherlands
§ Department of Pulmonary Diseases, University Medical Center Utrecht, 3584 CX Utrecht, The Netherlands
‖ Department of Pediatrics, University of California, San Francisco, California 94143, USA
¶ Division of Molecular Biology, H8, The Netherlands Cancer Institute, 1066 CX Amsterdam, The Netherlands
 # These authors contributed equally to this work

Reactive oxygen species are required for cell proliferation but can also induce apoptosis[1]. In proliferating cells this paradox is solved by the activation of protein kinase B (PKB; also known as c-Akt), which protects cells from apoptosis[2]. By contrast, it is unknown how quiescent cells that lack PKB activity are protected against cell death induced by reactive oxygen species. Here we show that the PKB-regulated Forkhead transcription factor FOXO3a (also known as FKHR-L1) protects quiescent cells from oxidative stress by directly increasing their quantities of manganese superoxide dismutase (MnSOD) messenger RNA and protein. This increase in protection from reactive oxygen species antagonizes apoptosis caused by glucose deprivation. In quiescent cells that lack the protective mechanism of PKB-mediated signalling, an alternative mechanism is induced as a consequence of PKB inactivity. This mechanism entails the activation of Forkhead transcription factors, the transcriptional activation of MnSOD and the subsequent reduction of reactive oxygen species. Increased resistance to oxidative stress is associated with longevity. The model of Forkhead involvement in regulating longevity stems from genetic analysis in *Caenorhabditis elegans*[3–6], and we conclude that this model also extends to mammalian systems.

Reactive oxygen species (ROS) are a primary cause of cellular damage that leads to cell death[1]. In proliferating cells, protection from cell death is mediated by activity of the phosphatidylinositol-3-OH kinase (PI(3)K)–PKB signalling pathway, which is dependent on the presence of glucose[2]. In the absence of PI(3)K–PKB signalling, the FOXO subfamily of Forkhead transcription factors, con-

† Present address: Ludwig Institute for Cancer Research, University of California San Diego, La Jolla, California 92093-0670, USA.

